Dislocated Epitaxial Islands

X. H. Liu, F. M. Ross, and K. W. Schwarz
IBM Watson Research Center, P.O. Box 218, Yorktown Heights, New York 10598
(Received 17 July 2000)

Dislocation networks observed in $CoSi_2$ islands grown epitaxially on Si are compared with the results of dislocation-dynamics calculations. The calculations make use of the fact that image forces play a relatively minor role compared to line tension forces and dislocation-dislocation interactions. Remarkable agreement is achieved, demonstrating that this approach can be applied more generally to study dislocations in other mesostructures.

PACS numbers: 61.72.Lk, 61.72.Ff, 68.55.Jk

The behavior of dislocations on the mesoscopic scale has been studied for many decades because of their role in determining the mechanical properties of materials. More recently, dislocations have also become a topic of interest in the manufacture of semiconductor heteroepitaxial films and semiconductor devices, where their appearance can cause serious performance problems. Although continuum dislocation theory is well developed, the dynamical behavior of dislocations is extremely complicated. Hence, numerical simulation programs are necessary to forge a link between theory and experiments. We describe the application of such a program to the study of dislocated $CoSi_2$ islands, which, because of their relatively simple geometries and the sophisticated experimental techniques which can be brought to bear on them, provide an ideal laboratory in which to study the behavior of dislocations in small structures. The eventual goal is to treat more complicated mesostructures in which dislocations are important. Among such structures are grains in crystals, semiconductor devices, and thin metal and semiconducting films.

The growth of $CoSi_2$ islands on Si has been extensively studied as a consequence of efforts to produce high quality $CoSi_2$ films for electronic applications [1]. Our own growth experiments were carried out in a Hitachi H-9000 transmission electron microscope, designed to achieve ultrahigh vacuum (2×10^{-10} Torr) at the specimen area and further modified to allow several types of deposition to take place under continuous observation. Details of the instrumentation and sample preparation have been given elsewhere [2,3]. Cobalt was evaporated directly onto a cleaned prethinned Si (111) substrate held at 850 °C, which was observed in plan view. The $CoSi_2$ islands grow epitaxially on the Si surface with the expected B-type orientation [4], in which the $CoSi_2$ shares a [111] axis with the Si surface normal but is rotated by 180° about this axis. Islands are triangular or hexagonal in shape, with a flat top and sides consisting of (111) facets (Fig. 1). While smaller islands grow pseudomorphically, larger islands eventually relieve their internal mismatch strain through the introduction of misfit dislocations at the $CoSi_2$/Si interface. Islands in the 50–100 nm radius range often show dislocations, although many islands 200–300 nm in radius remain coherently strained. It is probable that this variability is due to differences in island thickness, a parameter which was not measured directly during our experiments, but which could be estimated from the strength of the strain contrast. In our real-time observations, a segment of dislocation is first observed to appear near one of the corners and then to extend rapidly along the island-substrate perimeter before gliding into the central part of the island. An example is given in Fig. 1(a). Eventually, as more and more dislocations enter the island, elegant networks are formed as seen in Figs. 1(b) and 1(c). It is noteworthy that, whereas previous work has emphasized sessile grown-in $\frac{1}{6}[112]$ dislocations [4] as a relaxation mechanism, our observations demonstrate that, in the present case at least, $\frac{1}{2}[110]$ glide dislocations nucleated at the island edge and moving on glide planes parallel to the (111) interface are dominant.

In treating this system computationally, the goal is to introduce dislocations into a model of the island structure and to calculate their behavior as a function of time. For geometries larger than a few nanometers, this can be done with reasonable accuracy using equations derived from linear elastic theory [5]. In this approach, the displacement of a particular point on a dislocation during each time step is assumed to depend on the force acting at that point, which in turn depends on the local value of the stress tensor. What makes such calculations complicated is that, in addition to the stresses inherent to the mesostructure, the stress tensor now contains terms arising from the dislocations themselves. Thus, the forces acting to move the dislocations can be loosely separated into four kinds of contributions: (a) the stress fields inherent to the mesostructure, (b) local "line-tension" forces arising from the fact that a curved dislocation has a strong self-interaction, (c) dislocation-dislocation interactions, and (d) "image" forces arising from the need to satisfy boundary conditions at the mesostructure surfaces and interfaces.

The stress fields inherent to a given mesostructure can usually be determined by performing an initial 3D finite element or boundary element calculation. The dislocation-generated terms, on the other hand, must be recalculated every time the dislocation configuration changes. Recently

 0031-9007/00/85(19)/4088(4)$15.00 © 2000 The American Physical Society

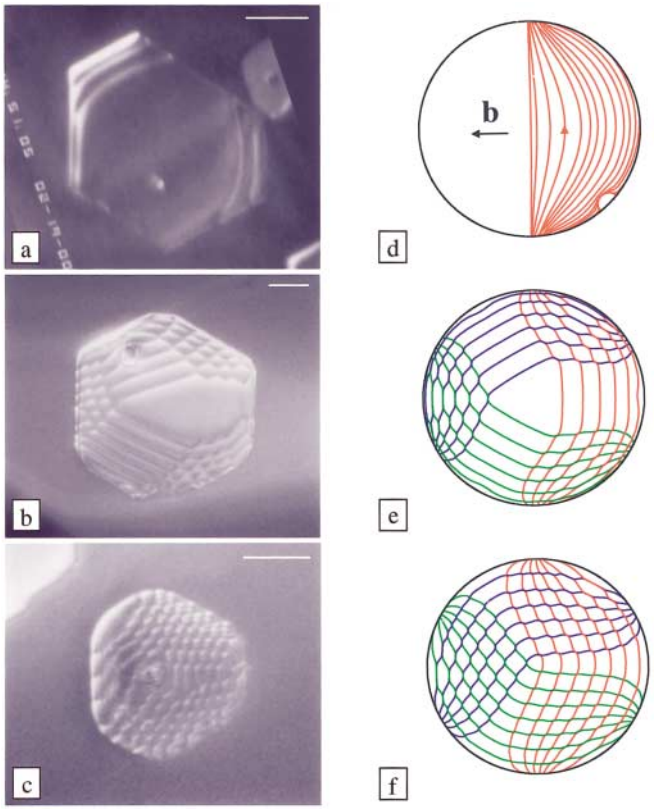

FIG. 1 (color). (111) plan-view of dislocations in $CoSi_2$ islands as observed by *in situ* transmission electron microscopy, and as simulated by 3D dislocation dynamics. The images were taken in a $\mathbf{g} = \langle 220 \rangle$ dark field condition for the Si substrate, showing the dislocations as lines of strong bright and dark contrast. The scale bar on each image represents 250 nm. (a) Initial entry of the dislocations, recorded at the growth temperature of 850 °C. (b) Observed configuration after holding the specimen at 850 °C for 30 min. (c) A second, smaller island, this time fully dislocated, recorded after cooling the specimen. The small circular features within each island are pinholes which form during growth. (d) Series of position snapshots showing the calculated evolution of a single $\mathbf{b} = \frac{1}{2}[110]$ dislocation loop introduced at the island edge. (e) Calculated transient configuration resulting from the introduction of six sets of dislocation loops, each containing the three possible $\frac{1}{2}[110]$ Burgers vectors for the (111) interface plane. (f) Fully relaxed pattern predicted by the simulations. Additional loops introduced into the island will not grow.

developed computer codes [6–9] can, in fact, do this in situations where the line-tension and dislocation-dislocation contributions are dominant. It is crucial to remember, however, that *all* such continuum codes replace the atomistic core structure by an approximate treatment of the self-interaction and are therefore subject to errors of order 10%–20%. Since the inherent stress fields in real mesostructures are also generally difficult to characterize very precisely, such a level of accuracy is the best that continuum dislocation dynamics calculations can realistically lay claim to.

This brings us to the image forces, the inclusion of which in large-scale dislocation simulations is straightforward in principle, but very difficult in practice. To compute

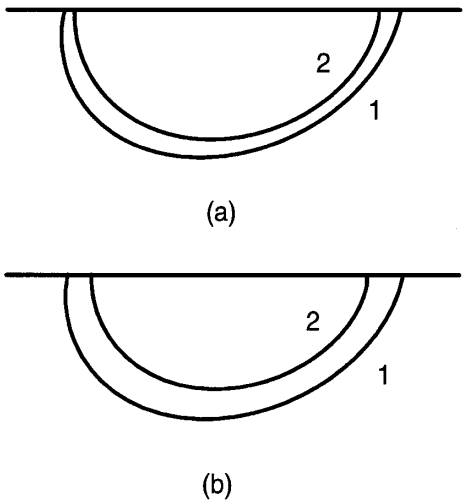

FIG. 2. Stationary loops intersecting a (001) free surface. The loops lie on the (111) plane and are viewed along the [110] direction. For both (a) and (b), curve 1 was calculated taking full account of the image fields; curve 2 was obtained ignoring them completely. (a) $\sigma_{xx} = \sigma_{yy} = 105$ MPa; the end points of curve 1 are 954 nm apart; (b) $\sigma_{xx} = \sigma_{yy} = 5.06$ GPa; the end points of curve 1 are 9.05 nm apart.

the fields which must be added to satisfy boundary conditions at the mesostructure surfaces requires a finite-element or boundary-element calculation at least as complicated as the initial inherent-field calculation. Unlike the inherent-field calculation, however, the image-force calculation must be repeated whenever the dislocation configuration changes significantly. Since a typical simulation requires hundreds of thousands of time steps, the computational load is increased to the point of impracticality.

How important are image corrections in the context of Figs. 1(a)–1(c), where dislocations are curving and interacting throughout the interior of a 1000 nm structure? To answer this question, we have investigated the simpler problem of dislocations interacting with a plane free surface, for which they can be evaluated accurately at every time step using the well-known Boussinesq-Cerruti formalism [10–12]. A detailed description of our numerical implementation of this formalism, and its applications, will be given elsewhere. For the present, we utilize this highly accurate calculation as a yardstick to demonstrate that, while image corrections are not insignificant, it is, in fact, sensible to neglect them as a first approximation when tackling the kind of problem illustrated in Fig. 1. As a particularly sensitive test relevant to Fig. 1, we show in Fig. 2 the calculated stationary (critical) configurations of surface loops subject to a uniform stress field, for loop sizes relevant to mesostructures [13]. Curves 1 in Figs. 2(a) and 2(b) show the results obtained when the image corrections are fully included, as can be seen from the fact that the ends have adjusted to approach the surface at the correct asymptotic angle. Curves 2 were obtained when image effects were entirely neglected [14]. One sees that for loops ranging from 10 to 1000 nm, the effect of the image corrections is of the same order as the 10%–20%

uncertainties inherent in any mesoscopic dislocation dynamics calculation. The image forces generated by curved surfaces will be of the same order as those arising from a flat surface. Given the enormous computational labor of including image corrections for more complicated geometries, their neglect can thus be justified as a practical first approximation.

Digressing for a moment, we remark that some workers are currently attempting to model dislocation image forces by means of finite-element calculations using rather coarse cell sizes. Our studies show that this is not appropriate for the kind of problem considered here, where the dislocations actually intersect the boundary. When this occurs, a divergence in the image force arises which must be regularized in the customary way, that is, by introducing a finite core thickness. To do this, we resolve the surface-grid points down to 0.01 nm near the intersect point and utilize the same Brown core-splitting procedure [15] that we use to handle the analogous problem of the divergent self-interaction. Just as the line-tension term arising from the core-averaged self-interaction dominates the bulk behavior of a dislocation, so does the regularized action of the image force on the line intersecting the surface dominate its surface behavior. Thus, we find that the differences between curves 1 and 2 in Figs. 2(a) and 2(b) arise almost entirely from image forces acting very near the boundary. Indeed, at the point farthest from the surface in curve 1 the image force is a totally insignificant 0.7% of the self-forces for Fig. 2(a) and is still only about 1.8% for the tiny loop in Fig. 2(b). For surface-intersecting dislocations, a finite-element (FEM) calculation which does not resolve the core region will capture only such small long-range corrections, while missing the dominant effect.

In order to interpret the observations in Figs. 1(a)–1(c), the islands were modeled as truncated cones, having a radius R at the interface and a height h. This allows the inherent stress fields to be calculated in a straightforward way using commercial software [16]. The dihedral angle between the sidewall of the cone and the interface was fixed at 70.5°, the angle between {111} planes. Since $CoSi_2$ has a smaller lattice constant than Si, it is under tension, leading to diverging stresses at the edge where the cone touches the Si surface. Figure 3 shows typical results for the shear stress very near the interface, which is the quantity of greatest interest here. We note particularly that, for a given aspect ratio h/R, the results are a universal function of r/R. Here, r is the distance from the island center. Thus, at a given distance $d = R - r$ from the edge, the stress *increases* as the island becomes larger. This implies that as the islands become larger, it should be easier to nucleate dislocations at the edge. In addition, we note from Fig. 3 that the interfacial stresses increase with aspect ratio, implying that thick islands will become dislocated sooner than thin structures.

Simulations of dislocation loops introduced in the edge region were carried out using the PARANOID code [8]. Image forces were neglected, in accord with the discussion given above. Since the interface normal is in the [111] direction, dislocation loops can nucleate in the edge region and glide towards the center of the island on the interface plane or on a (111) plane slightly above the interface. If one of the three possible $\frac{1}{2}[110]$ Burgers vectors is assigned to the dislocation, and the loop is allowed to evolve numerically, we find that it will first grow along the edge and then propagate towards the center, as shown in Fig. 1(d), eventually reaching a stationary configuration as a straight line along the diameter which is perpendicular to its Burgers vector. Because the initial growth occurs rapidly and unobservably close to the edge, it will seem as though the dislocation is growing into the island from a large part of the boundary at once, as is indeed observed [Fig. 1(a)]. If now more loops are introduced, the dislocations in the dot will interact with each other, as well as with the stress field of the island, resulting in the formation of elaborate network configurations within the island [17]. Two of the patterns predicted by our calculations are shown in Figs. 1(e) and 1(f), the latter depicting the limiting case of a fully relaxed island for which no additional dislocations can be introduced. Figures 1(b) and 1(c) show the corresponding situations as observed in the microscope.

As emphasized above, the calculations are subject to errors of 10%–20%. Within this context, however, the agreement of the predicted structures with experiment is as good as can be expected and certainly demonstrates the usefulness of the dislocation-dynamics approach. Even detailed features such as the increase in the line spacing towards the center of the island are qualitatively reproduced. The good agreement stems from three factors: (a) As is usually the case in 3D problems, line-tension forces are very important and, in fact, dominate the image effects to first order; (b) dislocation-dislocation interactions are also strong in this system, especially at the network nodes where the lines

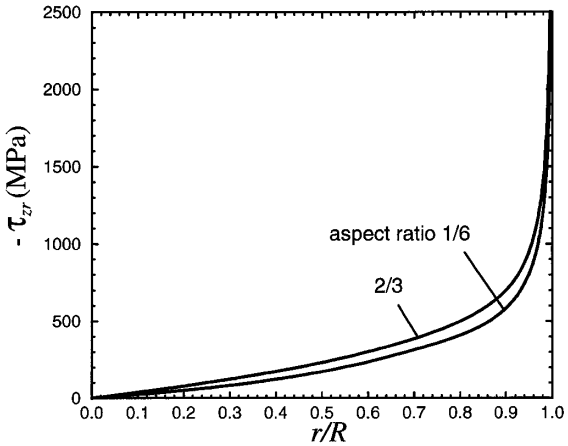

FIG. 3. Shear stress on the island/substrate interface, as a function of distance from the island center. Note that the stress diverges at the island perimeter and that it increases with island thickness.

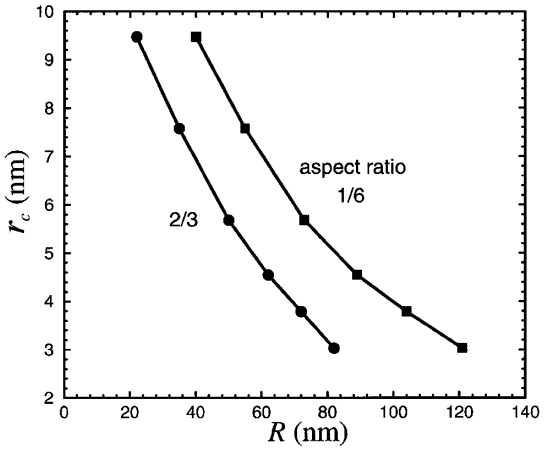

FIG. 4. Critical dislocation size (see text for discussion) as a function of island radius. For a given island, dislocations above the critical size will grow towards the center of the island, while those below will disappear.

pass by each other, and again are much larger than the image forces in most of the island; and (c) those parts of the dislocation configuration for which image forces are obviously important [e.g., the lines running along the perimeter in Fig. 1(e)] lie in regions where the stress diverges and the dislocation configuration is very insensitive to errors in the force calculation.

Since it becomes progressively easier to nucleate dislocation loops as an island grows, it is likely that it is the nucleation process rather than the critical size which determines when a given island will actually dislocate. While recognizing the limitations of the dislocation-dynamics approach at very small scales, some qualitatively useful information about the nucleation process can be obtained as follows. For a given R and h, variously configured nucleation loops can be introduced into the island and their subsequent evolution determined by direct simulation. In this way, it is easy to determine the stationary (critical) loop configuration through which the system must be activated if the island is to dislocate. Figure 4 shows the calculated neutral loop size as a function of island size for two values of the aspect ratio. Although only qualitative, these estimates are in accord with the observed behavior. That is, if one assumes that loops of radius 1–2 nm are easily nucleated, then thick islands will dislocate at $R \approx 100$ nm, while thin islands will need to become considerably larger before they do so.

In summary, we have shown that, in simulating dislocations in mesostructures, the difficult-to-compute image forces can often be neglected without greatly degrading the accuracy of the calculations. Because of this simplification, current dislocation-dynamics codes and 3D FEM stress tensor calculations can be combined to predict the observed dislocation patterns in complicated mesostructures with considerable fidelity. We have demonstrated the utility of this approach for the particular case of the dislocated island, for which the dislocation patterns have been observed in exceptional detail. In addition, we have shown how to obtain at least qualitative insight into the relevant nucleation mechanisms. This initial success implies that the same machinery can now be used to investigate other strained mesostructures.

The authors acknowledge stimulating and useful discussions with L. B. Freund, J. Tersoff, R. M. Tromp, and P. A. Bennett.

[1] K. Maex, Mater. Sci. Eng. **R11**, 53 (1993).
[2] M. Hammar, F. LeGoues, J. Tersoff, M. C. Reuter, and R. M. Tromp, Surf. Sci. **349**, 129 (1995).
[3] F. M. Ross, P. A. Bennett, R. M. Tromp, J. Tersoff, and M. C. Reuter, Micron **30**, 21 (1999).
[4] C. W. T. Bulle-Lieuwma, D. E. W. Vandenhoudt, J. Henz, N. Onda, and H. von Kanel, J. Appl. Phys. **73**, 3220 (1993).
[5] J. P. Hirth and J. Lothe, *Theory of Dislocations* (Krieger, Malabar, FL, 1992).
[6] B. DeVincre and L. P. Kubin, Model. Simul. Mater. Sci. Eng. **2**, 559 (1994).
[7] H. M. Zbib, M. Rhee, and J. P. Hirth, Int. J. Mech. Sci. **40**, 113 (1998).
[8] K. W. Schwarz, J. Appl. Phys. **85**, 108 (1999).
[9] N. M. Ghoniem and L. Z. Sun, Phys. Rev. B **60**, 128 (1999).
[10] M. C. Fivel, T. J. Gosling, and G. R. Canova, Model. Simul. Mater. Sci. Eng. **4**, 581 (1996). It should be noted that there are several misprints in the equations quoted in this paper.
[11] M. C. Fivel and G. R. Canova, Model. Simul. Mater. Sci. Eng. **7**, 753 (1999).
[12] A. Hartmaier, M. C. Fivel, G. R. Canova, and P. Gumbsch, Model. Simul. Mater. Sci. Eng. **7**, 781 (1999).
[13] The free surface calculations discussed in this section were for dislocation loops in silicon, lying on the (111) plane, with $\vec{b} = \frac{1}{2}[101]$. The surface normal is in the [001] direction.
[14] In this approximation, only the dislocations under the surface contribute to the field, and the surface point self-interaction is treated by a simple reflection procedure, as described in Ref. [8].
[15] L. M. Brown, Philos. Mag. **10**, 441 (1964).
[16] *ABAQUS User's Manual Version 5.7* (Hibbitt, Karlsson, and Sorensen, Inc., Pawtucket, RI, 1997). The materials constants used for this and for the dislocation-dynamics calculations were, for Si, unit cell dimension $a = 0.5433$ nm, shear modulus $\mu = 6.77 \times 10^{10}$ Pa, and Poisson ratio $\nu = 0.218$. For $CoSi_2$, the values used were $a = 0.5356$ nm, $\mu = 6.557 \times 10^{10}$ Pa, and $\nu = 0.22$.
[17] In order to avoid having to model junction formation, each set of Burgers vectors is injected on a different glide plane, the planes being spaced 5 atomic spacings apart. Thus the computed pattern has the nature of a dipole network. The appearance of the network depends only very weakly on the chosen dipole separation and, in fact, looks the same if junctions are allowed to form.